

Fig. 1. Optical reconstruction of a  $64 \times 64$  DBS hologram.

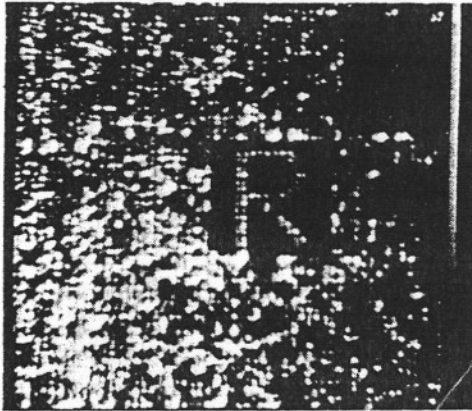


Fig. 2. Optical reconstruction of the  $64 \times 64$  DBS hologram in Fig. 1 replicated  $2 \times 2$  times.

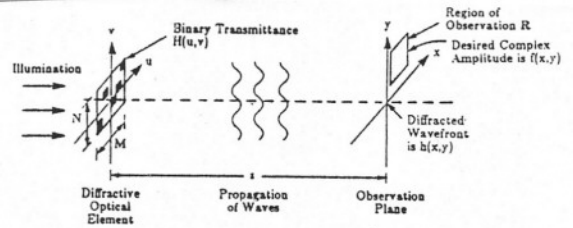


Fig. 3. Wavefront shaping with a binary CGH.

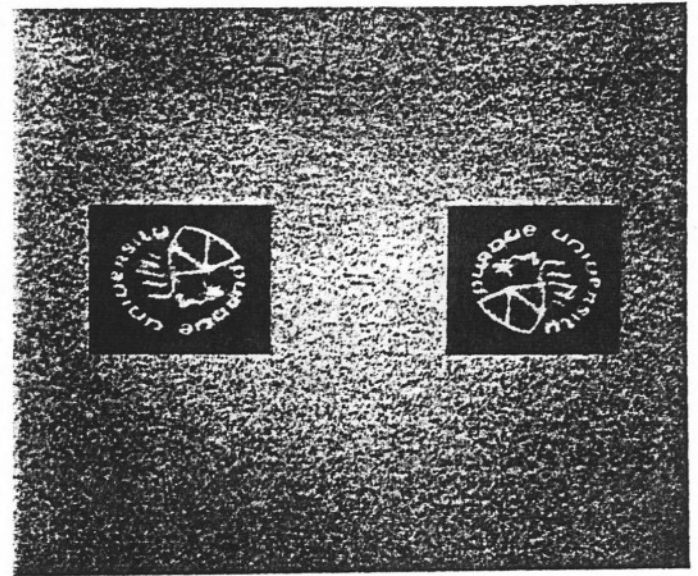


Fig. 5. Image reconstructed digitally from a  $512 \times 512$  DBS hologram.

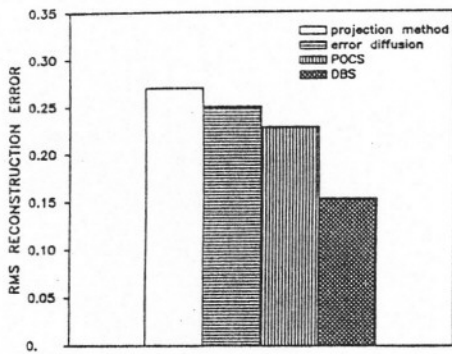


Fig. 7. Normalized rms error  $\bar{e}_{rms}$  for the four design methods investigated. The errors are averaged over the images reconstructed from  $64 \times 64$  holograms designed for the six objects in Fig. 6.

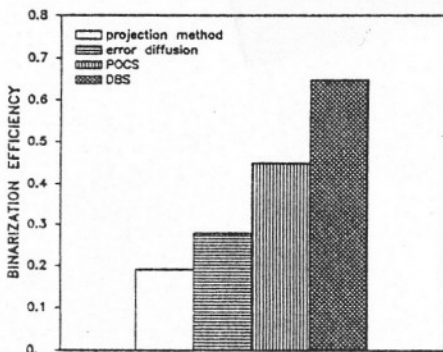


Fig. 8. Binarization efficiency  $\eta_{bin}$  for the four design methods investigated. The efficiencies are averaged over the images reconstructed from  $64 \times 64$  holograms designed for the six objects in Fig. 6.

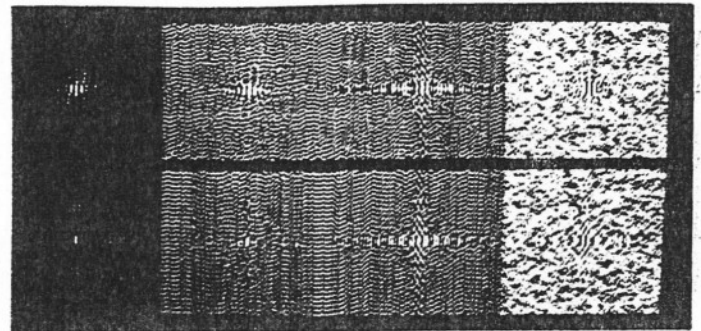


Fig. 9. Binary transmittance functions of  $128 \times 128$  holograms synthesized by the four methods for two different  $32 \times 32$  objects. From left to right, the holograms were designed by the projection method, error diffusion, POCS, and DBS.

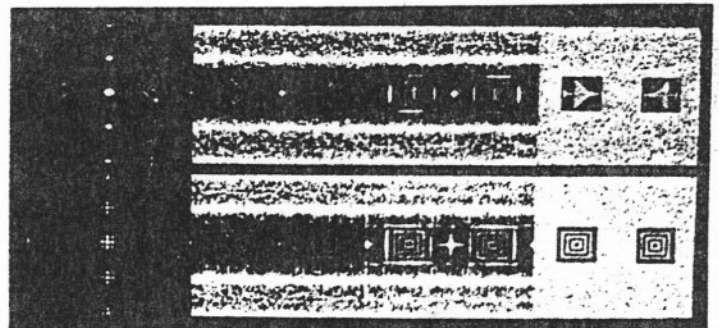


Fig. 10. Images reconstructed digitally from the  $128 \times 128$  holograms shown in Fig. 9.